行政院國家科學委員會專題研究計畫　期中進度報告

總計畫:下一世代無線行動接取技術(1/2)

計畫類別： 整合型計畫
計畫編號： NSC94-2213-E-009-055-
執行期間： 94 年 08 月 01 日至 95 年 07 月 31 日
執行單位： 國立交通大學電信工程學系(所)

計畫主持人： 蘇育德

計畫參與人員： 黃汀華、劉人仰、廖明&#22531；、陳青煒

報告類型： 精簡報告

處理方式： 本計畫可公開查詢

中　華　民　國 95 年 5 月 30 日

行政院國家科學委員會專題研究計畫成果報告

下一世代無線行動接取技術-總計畫

Next Generation Mobile Radio Access Technologies (1/2)

計畫編號：NSC 93-2218-E-009-015
執行期限：94 年 8 月 1 日至 95 年 7 月 31 日
主持人： 蘇育德　國立交通大學電信工程學系
計畫參與人員：黃汀華、劉人仰、廖明堃、陳青煒

中文摘要

在第三代的通訊系統技術已進入商業化的程序之後，無論是學界或工業界都已開始在討論著下一代的通訊系統 (Beyond Third Generation, B3G)的可能架構與技術。新一代的通訊系統(B3G)預期將提供更全面性的服務，包括高速的資料傳輸、多媒體服務及數據行動通訊，使無線通訊的產業更加蓬勃。

雖然下一代的通訊系統的完整架構仍在討論，但是我們可以確定的是 B3G 無線通訊系統的設計核心仍是在新的傳輸介面(Air Interface)，即無線接取技術(Wireless Access Technology)之確立。

本總計畫含括三個子計劃，計劃名稱分別為：

(1) 下一世代無線行動接取技術 - 子計劃一:多通道多速率展頻技術。

(2) 下一世代無線行動接取技術 - 子計畫三:時空信號處理及多用戶檢測。

(3) 下一世代無線行動接取技術 - 子計劃四:同步、通道估計與內接收機設計。

各個子計劃所發展的成果將在本報告中以獨立章節做一重點性的說明，並輔以軟體模擬成果以提供完整的系統性能評估之用。本報告為二年期計劃中第一年相關研究成果的總體精簡報告。

關鍵詞：無線通訊，行動無線接取技術，B3G。

Abstract

As the 3G systems have been deployed and commercialized, research institutes, major equipment providers as well as operators from all over the world had joined forces to look into future generations (beyond the third generation, B3G) of wireless communications, creating the Wireless World Research Forum (WWRF).

It is expected that the air interface will be playing the central role of the B3G wireless network. In this report, we propose a new broadband wireless mobile access architecture that is suitable for high-speed multimedia wireless transmission, predict its overall performance, and validate its feasibility. We produce simulation programs so that future users can emulate the performance of our joint design. This joint effort consists of tree sub-projects, namely,

1. Multi-channel multi-rate spreading sequences technologies.
3. Space-time signals processing and multi-user detection.
4. Synchronization, channel estimation and inner receiver design.

It is clear that each sub-project studies a vital part of a broadband wireless mobile

transmission system and all of them are closely coupled. For detailed description of each sub-project please refer to the sub-project reports.

Keywords: Wireless Communications, Mobile Radio Access Technologies, B3G.

1. Introduction

下一代新的無線接取技術到底為何，是繼續發展、改善 3G 的 CDMA 技術或需要新的接取技術，雖然以歐、日大廠的研發趨勢與成果來判斷後者的可能性較高，但現在尚無法確定。就目前的資料來看，基本的傳輸要求至少包括了：

(1). 低速環境傳輸率 > 155 Mbps

(2). 低速環境傳輸率 > 2 Mbps

(3). 系統容量 > 10 倍 3G 容量

要達到這個目標當然得要改善3G的傳輸技術。本計畫所從事研究之接取技術，係為目前無線寬頻通訊產、學業中積極發展，頗具潛力的研究課題，也是未來B3G 無線通訊系統運用所需建立的關鍵技術。我們研發的成果，累積的技術能量可提供業界諮詢，所培訓人員更可給予國內通訊產業運用。除此之外，本計畫所研究具備高效率、高彈性、高適應性的系統架構，可供完整的系統性能模擬、評估之用。

我們這個計畫分為三個子計畫，將分別就這些發展中技術做深入的研究。三個子計畫的名稱與主持人為：

一、下一世代無線行動接取技術：多通道多速率展頻技術（中興大學 楊谷章教授）

二、下一世代無線行動接取技術：時空信號處理及多用戶檢測（中興大學 翁芳標助理教授）

三、下一世代無線行動接取技術: 同步、通道估計與內接收機設計（交通大學 蘇育德教授）

以上三個子計畫在整個傳輸介面所探討的部分及互相之整合程度請參見各子計畫計畫書。綜合言之，各子計畫負責傳輸介面的一特定環節，互補性與相關性至為明顯，缺一不可。基本上，我們是以可調式多天線、多傳輸率的 OFDM/CDMA 系統為基礎架構。我們的研究成果除了可運用於 B3G 的行動通訊外，也旁及無線區域網路如 IEEE 802.11a、g，個人區域網路(Wireless Personal Area Network, WPAN)及廣域網路如 IEEE 802.16 等之應用。

在下列章節中，我們將就各子計劃去年的成果做一重點性說明。

2. 下一世代無線行動接取技術-子計劃一：多通道多速率展頻技術

2.1 Introduction

In the MC/DS-CDMA systems, the system performance gets worse as the multiple-access interference (MAI) increases. Therefore, a new class of two dimensional orthogonal variable spreading factor (2-D OVSF) codes [2] was proposed to eliminate the MAI by the mutual orthogonality between different users in the previous project. However, to maintain the code's orthogonality, the code cardinality of 2-D OVSF codes is restricted. Therefore, in order to support more subscribers and simultaneous users than the existing system using 2-D OVSF codes, a new 2-D non-orthogonal code, so-called frequency-hopping time-spreading codes are proposed in this project.

The new 2-D non-orthogonal codes which use Walsh codes and modified m-sequences for frequency-hopping, and Barker codes for time-spreading are proposed to increase the number of subscribers by utilizing two coding dimensions simulta-

neously. As a result, the overall code cardinality becomes a product of a quadratic function of the cardinality of the bipolar codes used for frequency hopping and a linear function of the cardinality of the bipolar codes used for time-spreading. Therefore, the overall code cardinality is improved substantially.

2.2 Constructions of the 2D Non-Orthogonal Codes

The 2-D frequency-hopping time-spreading codes (2-D FT codes) are obtained by the permutation of these multi-carrier codeword algebraically onto the time slots of another code chosen for time spreading. The algebraic permutation is controlled by prime sequences over Galois field of a prime number [3] in order to keep the cross-correlation functions of the resulting 2-D FT codes as low as possible. The best candidate that can serve as the time spreading bipolar code in our 2-D FT coding scheme is the family of Barker sequences [4]. The reason for choosing the Barker sequences as our time-spreading bipolar codes is because the maximum autocorrelation sidelobe of the barker sequence no more than one. The cross-correlation property is not that important because there exists only one Barker sequence that is used as the time spreading bipolar codeword for a given length. In other words, any bipolar codes with good autocorrelation property can also be used for time spreading in our 2-D FT codes.

The construction of the synchronized prime sequences begins with $\mathrm{GF}(p)$ of a prime number p, $S_{i,l} = (s_{i,l,0}, s_{i,l,1}, ..., s_{i,l,p-1})$, such that $s_{i,l,j} = (i \otimes j) \oplus l$, where i, j, and l are all in $\mathrm{GF}(p)$, "$\otimes$" denotes a modulo-p multiplication, and "$\oplus$" denotes a modulo-p addition. As a result, p^2 distinct synchronized prime sequences of length p are obtained. These p^2 sequences can be partitioned in p groups of p sequences each. The first sequence in each group is the original prime sequence, which generates other p-1 sequences in the group. The synchronized prime sequences have two correlation properties [3]: 1) the cross-correlation function is at most one for any two prime sequences originated from different groups; 2) the cross-correlation function only occurs at the auto- correlation peak position but the function can be as high as the autocorrelation peak for any two prime sequences originated from the same group.

To generate the 2-D FT code matrices, we are going to permute the multi-carrier bipolar codewords into the time slot of the time-spreading bipolar codeword in accordance to the prime sequences over a Galois field $\mathrm{GF}(p)$ for a prime p. Each sequence is used as a seed for generating a group of 2-D FT code matrices. The number of matrices in each group is determined by the number of available multi-carrier bipolar codewords (i.e., Φ_λ). The time-spreading bipolar codeword has the length n=p. By permuting these Φ_λ multi-carrier bipolar codewords onto the n time slots of the time-spreading bipolar codeword in accordance to the patterns of the prime sequences, this gives $\Phi_{group} = p$ groups of Φ_λ 2-D FT code matrices each and, thus, $\Phi_{FTC} = \Phi_{group}\Phi_\lambda = p^2$ 2-D FT code matrices in total.

The performance of 2-D FT codes will be better by selecting some special code matrices from our 2-D FT codes. It means there is no interference when the number of simultaneous users is less then p. Therefore, using the group property of the synchronous prime sequences, we can choose the group0 of matrices when the number of users is less than or equal to p; otherwise, we need to use multiple groups.

2.3 Performance Analysis

The average performance of the 2-D FT codes is analyzed and compared with that of 2-D OVSF codes and 2-D random codes in this section. The transmitter of the kth user

is shown in Fig. 1, where $k \in \{1,2,\ldots,K\}$ and K is the number of simultaneous users. We separate the total bandwidth into M orthogonal frequency bands of equal width. The binary data bit stream of the user k, $b_k(t)$, is multiplied by the code sequence $C_{k,m}$ of length N and is transmitted by the mth frequency carrier w_m, where $m \in \{1,2,\ldots,M\}$ and $C_{k,m}$ represents the mth row of the distinct 2-D code matrix of size $M \times N$ designated to user k, and M is the length of Walsh code.

The receiver of the kth user is shown in Fig. 2. By summing up all the MC/DS-CDMA signals at the receiver, the received signal is given by

$$r(t) = \sqrt{2P}\sum_{k=1}^{K}\sum_{m=1}^{M}\alpha_{k,m}b_k(t-\tau_k)C_{k,m}(t-\tau_k) \cdot \cos(\omega_m t + \theta_{k,m}) + n(t), \quad (1)$$

where $n(t)$ is AWGN with a double-sided power spectrum density (PSD) of $\eta_0/2$, τ_k is the transmitted delay of user k, $\alpha_{k,m}$ and $\theta_{k,m}$ are the amplitude and phase for user k in the mth channel, respectively. The MC/DS-CDMA signals detected at a receiver are first frequency-filtered into M diversity branches in accordance to the signals' carriers. The M filtered and despreaded signals $Z_{k,m}$ (for $m \in \{1,2,\ldots,M\}$), from a decision sample (per bit period) are then combined by a linear combiner, such that $Z = \sum_{m=1}^{M} Z_{k,m}$. In this project, the assumptions of perfect carrier, bit, chip synchronization and phase detections [1] are considered. The filtered, despreaded and sampled output Z at the receiver is given by

$$Z = S + I + \eta, \quad (2)$$

where S is the desired output of users, I is the despreaded interference term caused by other simultaneous users, and η is the filtered and despreaded AWGN term with a double sided PSD of $\eta_0/2$.

Assume that the MAI from other simultaneous users and the noise after despreading at the receiver are zero-mean Gaussian independent random variables. Then the mean of Z is given by

$$E[Z] = \pm\sqrt{P}T_b\sum_{m=1}^{M}\alpha_{1,m} \quad (3)$$

and the variances of Z is given by

$$VAR[Z] = VAR[\eta] + VAR[I], \quad (4)$$

where $VAR[\eta] = MT_b\eta_0/2$. Therefore, the signal-to-noise ratio (SNR) can be calculated and represented as [5], [6]

$$SNR = \frac{E^2[Z]}{VAR[Z]} = \frac{E^2[Z]}{VAR[I]+VAR[\eta]}. \quad (5)$$

In an AWGN channel, we can evaluate the error probability, P_e based on Gaussian approximation, which is given by

$$P_e = Q(\sqrt{SNR}), \quad (6)$$

where $Q(x) = (2\pi)^{-1/2}\int_x^\infty \exp(-z^2/2)dz$ is the Q-function.. In a Rayleigh fading channel, the average bit error probability P_e is given by [4]

$$P_e = \int_0^\infty Q(\sqrt{SNR(u)})\cdot f_u(u)du, \quad (7)$$

where $f_u(u) = \frac{u}{\sigma^2}e^{-\frac{u^2}{2\sigma^2}}$ is the Rayleigh distribution. Similarly, in a Rician fading channel, $f_u(u)$ in (7) can be represented as

$$f_u(u) = \frac{u}{\sigma^2}e^{-\frac{u^2+v^2}{2\sigma^2}}I_0\left(\frac{uv}{\sigma^2}\right), \quad (8)$$

where $I_0(x) = (2\pi)^{-1/2}\int_0^{2\pi}\exp(x\cos\theta)d\theta$ is the modified zero-order Bessel function of the first kind [4], the Rice parameter is defined as $v^2 + 2\sigma^2 = 1$ and $R \equiv v^2/2\sigma^2$.

We apply Gaussian approximation to calculate the variances of MAI of the 2-D FT codes. As discussed in Section 2.2, the 2-D FT codes support at most $\Phi_{FTC} = p^2$ matrices. Using the group property of the synchronous prime sequences, we can choose the group 0 of matrices when the number of users is less than or equal to p; otherwise, we need to use multiple groups. Thus, the average variance of the

cross-correlation functions of the 2-D FT codes is generally given by

$$\bar{\sigma}_g^2 = \left(\frac{p}{K} \times \bar{\sigma}_{g,p}^2 + \frac{K-p}{K} \times \bar{\sigma}_{g,jp}^2 \right), \quad (9)$$

where $2 \le j \le p$ is the number of groups in use. $\bar{\sigma}_{g,p}^2$ denotes the variance of the cross-correlation functions in group 0 when $\Phi_{FTC} = p$, such that

$$\bar{\sigma}_{g,p}^2 = 0. \quad (10)$$

Such condition occurs only in the desired user and interferers are using the synchronized prime sequences from the group 0. $\bar{\sigma}_{g,jp}^2$ denotes the variance of the cross-correlation functions when $\Phi_{FTC} > p$, such that [7]

$$\bar{\sigma}_{g,jp}^2 = \frac{1}{j} \times \left[\frac{(jp-p)\sigma_{p1}^2}{jp-1} \right] + \frac{j-1}{j} \times \left[\frac{(p-1)\sigma_{t1}^2}{jp-1} + \frac{(jp-p)\sigma_{p2}^2}{jp-1} \right], \quad (11)$$

where the first and second terms in (11) relate to the variances of the cross-correlation functions of the desired multicarrier codeword originated from group 0 and group i (for $i \in [1, p-1]$), respectively. σ_{p1}^2 is the variance of the cross-correlation functions created when the desired user and interferers are using the synchronized prime sequences from different groups. Thus, we have $\sigma_{p1}^2 = (K-1)\cdot\sigma_{t1}^2$. σ_{t1}^2 is the variance of the cross-correlation functions created when the desired user and interferers are using the synchronized prime sequences from the same group. We then have $\sigma_{t1}^2 = (K-1)/N$. $\sigma_{p2}^2 = (K-1)$ is derived similar to σ_{p1}^2.

The 2-D FT codes have the zero cross-correlation property, and thus, zero error probability. For supporting greater cardinality, we can always select more than group 0 of synchronized prime sequences and the variance in (11) gets worse as more groups are used (i.e., j increases). In other words, we should choose the group 0 of matrices when the number of users is less than or equal to p. For the number of users between p+1 and $\Phi_{FTC} = p^2$, we need to use multiple groups. For the case of the maximum cardinality of $\Phi_{FTC} = p^2$, the average variance [i.e., j=p in (11)] becomes

$$\bar{\sigma}_{g,jp}^2 = \frac{1}{p} \times \left[\frac{(p^2-p)\sigma_{p1}^2}{p^2-1} \right] + \frac{p-1}{p} \times \left[\frac{(p-1)\sigma_{t1}^2}{p^2-1} + \frac{(p^2-p)\sigma_{p2}^2}{p^2-1} \right]. \quad (12)$$

The variances of MAI of the 2-D FT codes, 2-D OVSF codes and 2-D random codes under the different channels are summarized in Table I.

2.4 Numerical Analysis

Figs. 3 and 4 show error probabilities versus the number of simultaneous users for 2-D FT codes, 2-D OVSF codes, and 2-D random codes in an AWGN channel, where SNR = 10 dB. In general, P_e gets worse as the number of the users K increases, but improves as a length of code N increases. From Fig. 3, we can find that the performance of 2-D FT codes is better than the performance of the 2-D random codes and worse than the performance of 2-D OVSF codes. Note that 2-D FT codes here support p times more matrices than the 2-D OVSF codes.

The difference between the Rician fading channel and Rayleigh fading channel is that the Rician fading has a line-of-sight (LOS), which will be determined by the parameter $R \equiv v^2/2\sigma^2$. A Rayleigh fading channel is the special case of a Rician fading channel with R=0. In these two channels, the orthogonality of the codes in the receiver's side would be partially destroyed or all destroyed due to the effects of phase change and amplitude fading. Figs. 5 and 6 show error probabilities versus the number of simultaneous users in a strong Rician fading and Rayleigh fading channels, where R=10 dB, SNR=10 dB. Figs. 7 and 8 show error

probabilities versus the number of simultaneous users in a weak Rician fading and Rayleigh fading channels, where R=5 dB, SNR=10 dB. From Figs. 5-8, we can find that the difference among the performance of these three codes will decrease as R decreases. In the extreme case (the Rayleigh fading channel), the performance of these three codes are almost the same.

2.5 Conclusions

In this project, we proposed 2-D FT codes which use Walsh codes and modified m-sequences for frequency-hopping and Barker codes for time-spreading. We also provided the performance analysis of 2-D FT codes, 2-D OVSF codes, and 2-D random codes under the AWGN, Rayleigh fading, and Rician fading channels. The results of our analysis showed that the proposed 2-D FT codes can support more number of subscribers than the 2-D OVSF codes with trade-off of the system performance.

3. 下一世代無線行動接取技術-子計畫三：時空信號處理及多用戶檢測

3.1 Introduction

Much research on spatial and temporal signal processing using an adaptive antenna array has been pursued in recent years[8]-[13]. The LMS algorithm requires less computation and its significant feature is simplicity, while the RLS algorithm provides a much faster convergence, and is relatively independent of the eigenvalues spread compared to the LMS algorithm [2]. Therefore, we will propose symbol-based adaptive antenna receiver structures without the need of calculation of the correlation matrix in this paper. We consider an MIMO-OFDM-DS/CDMA communication system similar to [14], which utilizes a transmit antenna array at the BS and a receive antenna array at the MS. However, our work is different from [14] because our adaptive receiver operates the transmit array, receiver antenna array, and OFDM block in multipath fading environments.

3.2 System Model

For MIMO-OFDM-DS/CDMA multiuser communication system including K users sharing a common frequency band, each user is assigned a unique spreading sequence $\mathbf{c}_k$ composed of Q chips at chip interval T_c which is equal to T_b/Q.

$$\mathbf{c}_k = \left[\mathbf{c}_1^{(k)} \quad \mathbf{c}_2^{(k)} \quad \cdots \quad \mathbf{c}_Q^{(k)}\right]^H, \mathrm{k} = 1,\cdots,\mathrm{K} \qquad (13)$$

where the superscript H represents the Hermitian transpose. In OFDM systems, a block of data of size Q where Q is a power of 2 is transmitted as an OFDM symbol. The base-band signal transmitted from the k-th user can be represented as

$$\begin{aligned}\mathbf{s}_t(n) &= \mathbf{F}^H \mathbf{c}_K \mathbf{d}_K(n),\ \mathrm{t} = 1,\cdots,\mathrm{N} \\ &= \left[s(Q(n-1)+1) \quad s(Q(n-1)+2) \quad \cdots \quad s(Q(n))\right]^T\end{aligned}$$

(14)

where $\mathbf{F}$ is the Fast Fourier transform (FFT) matrix. The IFFT matrix represents as $\mathbf{F}^H$ [9]. $d_k \in \{\pm 1 \pm \mathrm{j}\}$ is the data bit transmitted by k-th user under QPSK modulation, t means the tth transmitted antenna, and the superscript T means transpose. We consider a MIMO channel with N transmitted and M received antennas for a widely used discrete path physical model [15] and can be written as

$$\mathbf{H} = \sum_{p=1}^{P} \mathbf{h}_p \mathbf{a}_R(\theta_{M,p}) \mathbf{a}_T^H(\theta_{N,p}) = \mathbf{A}_R(\theta_M) \mathbf{H}_p \mathbf{A}_T^H(\theta_N)$$

(15)

where $\mathbf{H}$ is the channel matrix, $\mathbf{a}_T(\theta_N)$, $\mathbf{a}_R(\theta_M)$ are array steering by transmitter and receiver, respectively. The transmitter and receiver are coupled via P propagation paths with $\{\theta_{N,p}\}$ and $\{\theta_{M,p}\}$ as the spatial angles seen by the transmitter and receiver, respectively. The $\mathbf{H}_p$ represents the channel fading coefficient from p-th path. We suppose this channel model contains the effect of inter chip interference (ICI). L is the length of impulse response. So, we can construct a impulse response vector as $[a_1 \quad a_2 \quad \cdots \quad a_L]$. The channel $\breve{\mathbf{H}}$ can be rewritten as follows

$$\breve{\mathbf{H}} = \begin{bmatrix} \mathbf{H}_1 & 0 & \cdots & & 0 \\ \mathbf{H}_2 & \mathbf{H}_1 & 0 & \ddots & \vdots \\ \vdots & \mathbf{H}_2 & \ddots & & 0 \\ \mathbf{H}_L & \vdots & \ddots & & \mathbf{H}_1 \\ 0 & \mathbf{H}_L & \ddots & & \mathbf{H}_2 \\ \vdots & 0 & \ddots & & \vdots \\ \vdots & 0 & \ddots & & \vdots \\ 0 & \cdots & 0 & 0 & \mathbf{H}_L \end{bmatrix} \qquad (16)$$

where $\mathbf{H}_1 = a_1 \times \mathbf{H}$, $l = 1, \cdots L$. $\tilde{\mathbf{H}}$ is normalized $\breve{\mathbf{H}}$. Next, we represent the transmitted signal matrix **S**(n) as follows

$$\begin{aligned}\mathbf{S}(n) &= \begin{bmatrix}\mathbf{s}_1(n) & \mathbf{s}_2(n) & \cdots & \mathbf{s}_N(n)\end{bmatrix} \\ &= \begin{bmatrix} s_1(Q(n-1)+1) & s_2(Q(n-1)+1) & \cdots & s_N(Q(n-1)+1) \\ s_1(Q(n-1)+2) & s_2(Q(n-1)+2) & \cdots & s_N(Q(n-1)+2) \\ \vdots & \vdots & \ddots & \vdots \\ s_1(Qn) & s_2(Qn) & \cdots & s_N(Qn) \end{bmatrix} \\ &= \begin{bmatrix}\mathbf{z}_1(n) & \mathbf{z}_2(n) & \cdots & \mathbf{z}_Q(n)\end{bmatrix}^T\end{aligned}$$

$\mathbf{z}_q(n)$ is the *q*-th chip time signal of **S**(n). We rewrite transmitted signal matrix as

$$\mathbf{S}_q(n) = \begin{bmatrix} \mathbf{z}_{q-(2L-2)}(n) & \cdots & \mathbf{z}_{q-1}(n) & \mathbf{z}_q(n) \\ \vdots & \vdots & \vdots & \vdots \\ \mathbf{z}_{q-(2L-2)}(n) & \cdots & \mathbf{z}_{q-1}(n) & \mathbf{z}_q(n) \end{bmatrix}, \ \mathrm{q} = 1, \cdots, \mathrm{Q}$$

we make $\mathbf{S}_q(n)$ multiplied by $\tilde{\mathbf{H}}$

$$\mathbf{R}_q(n) = \tilde{\mathbf{H}}\mathbf{S}_q(n) + \mathbf{V}(n)$$

where **V**(n) is the zero mean and white Gaussian noise. The sum of elements on the diagonal of $\mathbf{R}_q(n)$ is what we want. Make $\mathbf{x}_q(n)$ represent the sum of elements on the diagonal of $\mathbf{R}_q(n)$. The baseband signal transmitted through channel can be represented as $\mathbf{x}_q(n)$.

3.3 Narrowband Adaptive Receiver

3.3.1 LMS-Based Receiver

In this subsection, we propose a MIMO-OFDM-DS/CDMA adaptive antenna receiver. As we mentioned before, antenna array is a appropriate description to MIMO channel model. The weight vector of the adaptive antenna is denoted as

$$\mathbf{w}_{LMS,k}(n) = \begin{bmatrix} w_0^{(k)} & w_1^{(k)} & \cdots & w_{M-1}^{(k)} \end{bmatrix}^H \qquad (17)$$

The received signal matrix as

$$\mathbf{U}(n) = \begin{bmatrix}\mathbf{x}_1(n) & \mathbf{x}_2(n) & \cdots & \mathbf{x}_Q(n)\end{bmatrix} \qquad (18)$$

Obviously, each element in the received signal matrix **U**(n) is QPSK signal. We get the despreader output sequence $d_{e,LMS,k}(n)$ and can be described as

$$d_{e,LMS,k}(n) = \mathbf{c}_k^H \mathbf{F}\mathbf{U}^H(n)\mathbf{w}_{LMS,k}(n)/Q \qquad (19)$$

where $d_{e,LMS,k}(n)$ is the received signal sequence of the desired user. The cost function of adaptive algorithm known as the complex LMS algorithm is the expected value of signal error. So, the cost function can be represented as follows:

$$\begin{aligned} J_{LMS} &= E\left[\left|d_k(n) - \mathbf{c}_k^H \mathbf{F}\mathbf{U}^H(n)\mathbf{w}_{LMS,k}(n)/Q\right|^2\right] \\ &= E\left[\left|e_{LMS,k}(n)\right|^2\right] \end{aligned} \qquad (20)$$

where $d_k(n)$ represents the original transmitted signal of the desired user at time instant n [10]. We assume that $d_k(n)$ is known in training period, and we call it as a pilot sequence which is transmitted before data transmission in most wireless communication system. According to the derivation of the LMS algorithm, we can recompose the cost function (20) as the following

$$\begin{aligned} E\left[\left|e_{LMS,k}(n)\right|^2\right] = E\Big[&\mathbf{w}_{LMS,k}^H(n)\mathbf{U}(n)\mathbf{F}\mathbf{c}_k\mathbf{c}_k^H\mathbf{F}\mathbf{U}^H(n)\mathbf{w}_{LMS,k}(n)/Q^2 \\ &- d_{e,LMS,k}^*(n)\mathbf{c}_k^H\mathbf{F}\mathbf{U}^H(n)\mathbf{w}_{LMS,k}(n)/Q \\ &- \mathbf{w}_{LMS,k}^H(n)\mathbf{U}(n)\mathbf{F}\mathbf{c}_k\mathbf{d}_k(n)/Q \\ &+ d_k(n)d_k^*(n)\Big] \end{aligned} \qquad (21)$$

where "*" means conjugate. It is no doubt that J_{LMS} is a complex value. In order to adaptively update the weight of the proposed receiver, we make a weight differential operation for cost function. We compute the gradient of the above cost function and then obtain

$$\frac{\partial J_{LMS}}{\partial \mathbf{w}_{LMS,k}} = -2\mathbf{U}(n)\mathbf{F}^H\mathbf{c}_k\mathbf{e}_{LMS,k}(n)/Q \qquad (22)$$

where $e_{LMS,k}(n)$ denotes the error for the desired user. Then, the weight vecor of the proposed receiver can be updated as follows,

$$\mathbf{w}_{LMS,k}(n+1) = \mathbf{w}_{LMS,k}(n) - \mu\frac{\partial J_{LMS}}{\partial \mathbf{w}_{LMS,k}} \qquad (23)$$

where μ is the step size.

3.3.2 Narrowband Adaptive Receiver with Code Adjustment

In this subsection, we propose a new idea about adaptive receiver. It is to apply adaptive operation on spreading code. In traditional CDMA system, spreading code is an invariant sequence with fixed coefficients ±1 and has strong orthogonally. When spreading code sequence was transmitted through fading channel, it's orthogonally would be ruined. So, we set up a new structure for code adjustment. The proposed receiver structure bases on LMS algorithm updates not only the weight vector of the MIMO-OFDM-DS/CDMA adaptive antenna receiver but also updates the despreading code coefficients. The elements of the despreading code are no longer ±1. According to the code update operation, the spreading code vector of the desired user should be defined as

$$\mathbf{c}_{LMS,k}(n)=\left[\mathbf{c}_1^{(k)}(n)\quad \mathbf{c}_2^{(k)}(n)\quad \cdots\quad \mathbf{c}_Q^{(k)}(n)\right] \tag{24}$$

the cost function can be represented like J_{LMSCA} as following:

$$\begin{aligned} J_{LMSCA} &= E\left[\left|d_k(n)-\mathbf{c}_{LMS,k}^H\mathbf{F}\mathbf{U}^H(n)\mathbf{w}_{LMS,k}(n)/Q\right|^2\right] \\ &= E\left[\mathbf{c}_{LMS,k}^H\mathbf{F}\mathbf{U}^H(n)\mathbf{w}_{LMS,k}(n)\mathbf{w}_{LMS,k}^H(n)\mathbf{U}(n)\mathbf{F}\mathbf{c}_{LMS,k}/Q^2\right. \\ &\quad -d_k^*(n)\mathbf{c}_{LMS,k}^H\mathbf{F}\mathbf{U}^H(n)\mathbf{w}_{LMS,k}(n)/Q \\ &\quad -\mathbf{w}_{LMS,k}^H(n)\mathbf{U}(n)\mathbf{F}^H\mathbf{c}_{LMS,k}\mathbf{d}_k(n)/Q \\ &\quad \left.+d_k(n)d_k^*(n)\right] \end{aligned} \tag{25}$$

Take gradient of the cost function by the code vector we obtain

$$\frac{\partial J_{LMSCA}}{\partial \mathbf{c}_{LMS,k}}=-2\mathbf{F}\mathbf{U}^H(n)\mathbf{w}_{LMS,k}(n)\mathbf{e}_{LMSCA,k}^*(n)/Q \tag{26}$$

where $e_{LMSCA,k}$ denotes the error for the desired user. The update equation of the weight vector for this receiver is the same as

$$\mathbf{w}_{LMS,k}(n+1)=\mathbf{w}_{LMS,k}(n)-2\mu_{n\_w}\frac{\partial J_{LMS}}{\partial \mathbf{w}_{LMS,k}} \tag{27}$$

The update equation of the despreader vector coefficients for this receiver is shown as follows

$$\mathbf{c}_{LMS,k}(n+1)=\mathbf{c}_{LMS,k}(n)-2\mu_{n\_c}\frac{\partial J_{LMSCA}}{\partial \mathbf{c}_{LMS,k}} \tag{28}$$

3.3.3 RLS-Based Receiver

Generally, recursive least squares (RLS) filter is faster than LMS filter in aspect of convergence speed. However, it is a tradeoff between convergence speed and computational complexity. The computation complexity of recursive least squares filter are more than LMS filter. The update equation of weight vector and code vector coefficients for RLS algorithm will be derived in following paragraph. Just like what we define in the above section, the weight vector for RLS algorithm is denoted as $\mathbf{w}_{RLS,k}(n)$ as follow

$$\mathbf{w}_{RMS,k}(n)=\left[\mathbf{w}_0^{(k)}(n)\quad \mathbf{w}_1^{(k)}(n)\quad \cdots\quad \mathbf{w}_{M-1}^{(k)}(n)\right]^H$$

We get the despreader output sequence $d_{e,RLS,k}(n)$ and can be described as

$$d_{e,RLS,k}(n)=\mathbf{c}_k^H\mathbf{F}\mathbf{U}^H(n)\mathbf{w}_{RLS,k}(n)/Q$$

Define the least squares cost function as the following,

$$\begin{aligned} J_{RLS} &= \sum_{i=1}^{n}\lambda^{n-i}\left\|d_k(i)-\mathbf{c}_k^H\mathbf{F}\mathbf{U}^H(n)\mathbf{w}_{RLS,k}(n)/Q\right\|^2 \\ &= \sum_{i=1}^{n}\lambda^{n-i}\left\|e_{RLS,k}(i)\right\|^2 \end{aligned} \tag{29}$$

where λ is the forgetting factor, and $e_{RLS,k}(n)$ denotes the error vector for the desired user. In order to derive the weight update equation for RLS algorithm, it is necessary to compute $\frac{\partial J_{RLS}}{\partial \mathbf{w}_{RLS,k}}=0$. Then, compute the gradient of the above cost function and then obtain

$$\frac{\partial J_{RLS}}{\partial \mathbf{w}_{RLS,k}} = \sum_{i=1}^{n} \lambda^{n-i} \left[2\mathbf{U}(i)\mathbf{F}\mathbf{c}_k \mathbf{c}_k^H \mathbf{F}\mathbf{U}^H(i)\mathbf{w}_{RLS,k}(n)/Q^2 - 2\mathbf{U}(i)\mathbf{F}^H \mathbf{c}_k d_k(i)/Q \right]$$

and make $\frac{\partial J_{RLS}}{\partial \mathbf{w}_{RLS,k}} = 0$

$$\Rightarrow \sum_{i=1}^{n} \lambda^{n-i}\, \mathbf{U}(i)\mathbf{F}\mathbf{c}_k \mathbf{c}_k^H \mathbf{F}\mathbf{U}^H(i)\mathbf{w}_{RLS,k}(n)/Q = \sum_{i=1}^{n} \lambda^{n-i} \mathbf{U}(i)\mathbf{F}^H \mathbf{c}_k \mathbf{d}_k(i) \quad (30)$$

The optimum weight of the adaptive filter ahs the form

$$\mathbf{w}_{RLS,k}(n) = Q\boldsymbol{\Phi}_w^{-1}(n)\mathbf{z}_w(n) \quad (31)$$

where $\boldsymbol{\Phi}_w(n)$ represents correlation matrix and $\mathbf{z}_w(n)$ represents cross-correlation vector. $\boldsymbol{\Phi}_w(n)$ and $\mathbf{z}_w(n)$ are described as the following,

$$\boldsymbol{\Phi}_w(n) = \sum_{i=1}^{n} \lambda^{n-i} \mathbf{U}(i)\mathbf{F}\mathbf{c}_k \mathbf{c}_k^H \mathbf{F}\mathbf{U}^H(i) + \delta\lambda^i \mathbf{I}_M \quad (32)$$

$$\mathbf{z}_w(n) = \sum_{i=1}^{n} \lambda^{n-i} \mathbf{U}(i)\mathbf{F}^H \mathbf{c}_k \mathbf{d}_k(i) \quad (33)$$

where $\mathbf{I}_M$ is the *M*-by-*M* identity matrix and δ is the regularization parameter. Using matrix-inversion lemma and the definition $\mathbf{P}_w(n) = \boldsymbol{\Phi}_w^{-1}(n)$, we obtain

$$\mathbf{P}_w(n) = \frac{1}{\lambda}\left[\mathbf{P}_w(n-1) - \mathbf{k}_w(n)\mathbf{c}_k^H \mathbf{F}\mathbf{U}^H(n)\mathbf{P}_w(n-1)\right] \quad (34)$$

where

$$\mathbf{K}_w(n) = \frac{\lambda^{-1}\mathbf{P}_w(n-1)\mathbf{U}(n)\mathbf{F}^H \mathbf{c}_k}{1+\lambda^{-1}\mathbf{U}(n)\mathbf{F}^H \mathbf{c}_k \mathbf{P}_w(n-1)\mathbf{c}_k^H \mathbf{F}\mathbf{U}^H(n)} = \mathbf{P}_w(n)\mathbf{U}(n)\mathbf{F}^H \mathbf{c}_k \quad (35)$$

is the Kalman gain vector. Substitute (33) into (21) we can get substituting (34) for $\mathbf{P}_w(n)$, and using (35) we get

$$\mathbf{w}_{RLS,k}(n) = \mathbf{w}_{RLS,k}(n-1) + \mathbf{K}_w Q\boldsymbol{\Omega}_w(n)$$

where $\boldsymbol{\Omega}_w = \mathbf{d}_k(n) - \mathbf{c}_k^H \mathbf{F}\mathbf{U}^H(n)\mathbf{w}_{RLS,k}(n-1)/Q$ is the prior estimation error.

3.4 Simulation Results and conclusion

In this section, we show some simulation results of our proposed adaptive receiver structures, as Fig. 9 shown. Before revealing the simulation results, there are some parameters about most following simulation results : uptx = 2 ～ 4 (the user number in each transmitted antenna branch), N = 4 (transmitted antenna number), M = 8 (Received antenna number). Furthermore, the data bits are transmitted with QPSK modulation. For LMS-based receiver structures, the step sizes for weight update equation are chosen from 0.02 to 0.001, and the step sizes for code update equation are chosen from 0.001 to 0.0001. For RLS-based receiver structures, we set the forgetting factor λ as 1. The spreading code we use is a set of Gold sequences with length Q = 31. From Figs.10 to Fig. 11, we find that the performances of the proposed RLS-based receivers are better than that of LMS-based receivers. Obviously, the performances of the system go down with the user number increasing in each transmitted antenna branch and Ec/N0 decreasing. The reason is the narrowband adaptive receiver with code adjustment can reduce the effect of ICI and with less noise enhancement effect. The simulation results also show that when the Wiener code filter is employed, the performance is always better than that without using it.

4. 下一世代無線行動接取技術-子計劃四：同步、通道估計與內接收機設計

4.1 Introduction

Orthogonal frequency division multiplexing (OFDM) is a popular modulation scheme for high-speed broadband wireless transmission [16], [17]. It popularity derives mainly from its capability to combat frequency selective fading as intersymbol interference (ISI) caused by multipath delay spread can be easily eliminated. The former adopts the Multiple Input Multiple Output (MIMO) technique to enhance the capacity, where MIMO refers to systems that have multiple transmit antennas and multiple receive antennas. Depending on the MIMO channel condition, the capacity of MIMO system increases with the number of transmitter and receive antennas. Recent developments in MIMO techniques promise a great boost in performance for OFDM systems.

With all its merits, OFDM, however, is sensitive to the carrier frequency offset (CFO) caused by Doppler shifts or instabilities of and mismatch between transmitter and receiver oscillators [18]. Depending on the application, the offset can be as large as many tens subcarrier spacing, and is usually divided into integer and fractional CFO parts.

The presence of a fractional CFO causes reduction of amplitude of desired subcarrier and induces inter-carrier interference (ICI) because the desired subcarrier is no long sampled at the zero-crossings of its adjacent carriers' spectrum. If the fractional CFO part can be perfectly compensated, the residual integer CFO does not degrade the signal quality but still results in circular shifts of the desired output, causing decision errors.

In this report, we extend Moose's ML CFO estimation algorithm for use in a multiple-antenna environments, assuming two identical pilot symbols are available. In addition, we extend the Yu and Su's ML CFO estimation algorithm that uses multiple repetitive pilot symbols.

4.2 System Model

Consider a frequency selective fading channel associated with a MIMO system of M_T transmit and M_R receive antennas. The equivalent time-domain baseband signal at the output of the *i*th receive antenna, $y_i[n]$, is given by

$$y_i[n] = \sum_{j=1}^{M_T} r_{i,j}[n] + w_i[n];\ n = 1, 2, ..., N;\ i = 1, 2, ..., M_R \quad (36)$$

where $\{w_i[n]\}$ is a complex additive whit Gaussian noise (AWGN) sequence and

$$r_{i,j}[n] = \frac{1}{N} \sum_{k \in D_j} \sqrt{\frac{E_s}{M_T}} S_j[k] H_{i,j}[k] e^{j2\pi n(k+\epsilon)/N} \quad (37)$$

is the part of the OFDM signal received by the *i*th receive antenna contributed by the *j*th transmit antenna. Moreover,

- $S_j[k]$ represents the symbol carried by the *k*th subcarrier at the *j*th transmit antenna.
- $H_{i,j}[k]$ is the channel transfer function between the *i*th receive antenna and the *j*th transmit antenna at the *k*th subcarrier.
- ε denotes the relative carrier frequency offset of the channel (the ratio of the actual

frequency to the intercarrier spacing).

- D_j is the set of modulated subcarrier for the *j*th transmit antenna.
- E_s is the average energy allocated to the *k*th subcarrier evenly divided across the transmit antennas.
- $\{h_{i,j}[n]\}$ and $H_{i,j}[k] = \sum_{n=0}^{L-1} h_{i,j}[n] e^{-\frac{j2\pi kn}{N}}$ are the channel impulse and frequency response between the *i*th receive antenna and the *j*th transmit antenna at the *k*th subcarrier.
- L is the maximum channel memory of all $M_T M_R$ SISO component channels.

Fig. 12 plots the transmission channel model for the *i*th receive antenna with respect to the MT transmit antennas. Rewriting (2.1) in matrix form

$$\begin{pmatrix} y_1[n] \\ y_2[n] \\ \vdots \\ y_{M_R}[n] \end{pmatrix} = \frac{1}{N} \sum_{k \in D_j} \sqrt{\frac{E_s}{M_T}} \begin{pmatrix} H_{1,1}[k] & H_{1,2}[k] & \cdots & H_{1,M_T}[k] \\ H_{2,1}[k] & H_{2,2}[k] & \cdots & H_{2,M_T}[k] \\ \vdots & \vdots & \ddots & \vdots \\ H_{M_R,1}[k] & \cdots & \cdots & H_{M_R,M_T}[k] \end{pmatrix} e^{j2\pi m(k+\varepsilon)/N} + \begin{pmatrix} w_1[n] \\ w_2[n] \\ \vdots \\ w_{M_R}[n] \end{pmatrix} \tag{38}$$

and using the substitutions

$$\begin{aligned} \mathbf{y}[n] &= (y_1[n]\ y_2[n]\ \cdots\ y_{M_R}[n])^T \\ \mathbf{S}[k] &= (S_1[k]\ S_2[k]\ \cdots\ S_{M_T}[k])^T \\ \mathbf{H}[k] &= [H_{i,j}[k]] \\ \mathbf{w}[n] &= (w_1[n]\ w_2[n]\ \cdots\ w_{M_R}[n])^T \end{aligned}$$

we obtain

$$\mathbf{y}[n] = \frac{1}{N} \sum_{k \in D_j} \sqrt{\frac{E_s}{M_T}} \mathbf{H}[k]\mathbf{S}[k] e^{j2\pi n(k+\epsilon)/N} + \mathbf{w}[n] \tag{4}$$

Let ε_f and ε_i be respectively the fractional and integer parts of the CFO so that $\varepsilon = \varepsilon_f + \varepsilon_i$ and define

$$\begin{aligned} Y[k] &= \sqrt{\frac{E_s}{M_T}} \sum_{m \in D_j} H[m]S[m] \left(\frac{1}{N} \sum_{n=0}^{N-1} e^{j2\pi(m+\varepsilon_f+\varepsilon_i)n/N} e^{-j2\pi kn/N} \right) + W[k] \\ &= \sqrt{\frac{E_s}{M_T}} H[k-\varepsilon_i]S[k-\varepsilon_i] \left(\frac{1}{N} \sum_{n=0}^{N-1} e^{-j2\pi\varepsilon_f n/N} \right) \\ &\quad + \sqrt{\frac{E_s}{M_T}} \sum_{\substack{m \in D_j \\ m \neq k-\varepsilon_i}} H[m]S[m] \left(\frac{1}{N} \sum_{n=0}^{N-1} e^{j2\pi(m+\varepsilon_i-k)n/N} e^{j2\pi\varepsilon_f n/N} \right) + W[k] \\ &= \sqrt{\frac{E_s}{M_T}} \underbrace{H[k-\varepsilon_i]S[k-\varepsilon_i]}_{\text{circular shift}} \underbrace{\left(\frac{1}{N} \frac{\sin(\pi\varepsilon_f)}{\sin(\pi\varepsilon_f/N)} e^{-j2\pi\varepsilon_f(N-1)/N} \right)}_{\text{reduction of the desired subcarrier}} \\ &\quad + \underbrace{\sqrt{\frac{E_s}{M_T}} \sum_{\substack{m \in D_j \\ m \neq k-\varepsilon_i}} H[m]S[m] \left(\frac{1}{N} \frac{\sin(\pi(\varepsilon_f+\varepsilon_i))}{\sin(\pi(m-k+\varepsilon_f+\varepsilon_i)/N)} e^{j\pi(\varepsilon_f+\varepsilon_i)(N-1)/N} e^{-j\pi(m-k)/N} \right)}_{ICI} \\ &\quad + W[k] \end{aligned} \tag{39}$$

It is clear that the presence of a fractional CFO causes reduction of the desired subcarrier's amplitude and induces inter-carrier interference (ICI). If the fractional CFO part can be perfectly compensated for, the integer CFO, if exists, will result in a circular shift of the desired output, causing decision errors.

4.3 Maximum Likelihood Estimate of CFO

4.3.1 Generalized Moose Estimate

Let *D* be the set of modulated subcarrier (indexes) that bear a pseudonoise (PN) sequence on the even frequencies and zeros on the odd frequencies. The resulting time-domain training sequence has two identical halves

$$r[n] = \frac{1}{N} \sum_{k \in D_e} \sqrt{\frac{E_s}{M_T}} H[k]S[k] e^{j2\pi n(k+\varepsilon)/N} \tag{40}$$

$$\begin{aligned} r[n+N/2] &= \frac{1}{N} \sum_{m \in D_e} \sqrt{\frac{E_s}{M_T}} H[k]S[k] e^{j2\pi(n+N/2)(k+\varepsilon)/N} \\ &= \frac{1}{N} \sum_{m \in D_e} \sqrt{\frac{E_s}{M_T}} H[k]S[k] e^{j2\pi n(k+\varepsilon)/N} e^{j2\pi\frac{N}{2}(k+\varepsilon)/N} \\ &= r[n] e^{j2\pi\varepsilon/2} \quad , \quad n = 1, 2 \ldots, N/2 \end{aligned}$$

(41)

where $\left(r_1[n] \quad r_2[n] \quad \cdots \quad r_{M_R}[n]\right)^T$ and D_e is the subset of even numbers in D.

Taking into account the AWGN term, we obtain

$$y[n] = r[n] + w[n] \tag{42}$$

$$y[n+N/2] = r[n]e^{j2\pi\varepsilon/2} + w[n+N/2] \tag{43}$$

where $\left(w_1[n] \quad w_2[n] \quad \cdots \quad w_{M_R}[n]\right)^T$. As illustrated in Fig 13, we define

$$\bar{\mathbf{y}}_1[i] = (y_i[1]\ y_i[2]\ \cdots\ y_i[N/2])$$

$$\bar{\mathbf{r}}_1[i] = (r_i[1]\ r_i[2]\ \cdots\ r_i[N/2])$$

$$\bar{\mathbf{w}}_1[i] = (w_i[1]\ w_i[2]\ \cdots\ w_i[N/2])$$

and

$$\bar{\mathbf{y}}_2[i] = (y_i[N/2+1]\ y_i[N/2+2]\ \cdots\ y_i[N])$$

$$\bar{\mathbf{r}}_2[i] = (r_i[N/2+1]\ r_i[N/2+2]\ \cdots\ r_i[N])$$

$$\bar{\mathbf{w}}_2[i] = (w_i[N/2+1]\ w_i[N/2+2]\ \cdots\ w_i[N])$$

where the subscript indicates either the first or the second half of a time-domain OFDM frame and the indexes within the bracket denotes from which receive antenna the time domain sample is derived. (42) and (43) then have the simplified expressions

$$\bar{\mathbf{y}}_1[i] = \bar{\mathbf{r}}_1[i] + \bar{\mathbf{w}}_1[i] \tag{44}$$

$$\bar{\mathbf{y}}_2[i] = \bar{\mathbf{r}}_1[i]e^{j2\pi\epsilon/2} + \bar{\mathbf{w}}_2[i] \tag{45}$$

The ML estimate of the parameter ε, given the received vector $\left(\bar{y}_1[i], \bar{y}_2[i]\right)$, is obtained by maximizing the likelihood function

$$f\left(\bar{y}_1[i], \bar{y}_2[i] \mid \varepsilon\right) = f\left(\bar{y}_2[i] \mid \bar{y}_1[i], \varepsilon\right) f\left(\bar{y}_1[i] \mid \varepsilon\right) \tag{46}$$

where we have denoted various conditional probability density functions by similar functional expressions, $f(.|.)$. As ε gives no explicit information about $\bar{y}_1[i]$, i.e. $f\left(\bar{y}_1[i] \mid \varepsilon\right) = f\left(\bar{y}_1[i]\right)$, the ML estimate of ε is given by

$$\begin{aligned} \hat{\varepsilon} &= \arg\max_{\varepsilon} f\left(\bar{y}_2[i] \mid \bar{y}_1[i], \varepsilon\right) f\left(\bar{y}_1[i] \mid \varepsilon\right) \\ &= \arg\max_{\varepsilon} f\left(\bar{y}_2[i] \mid \bar{y}_1[i], \varepsilon\right) \end{aligned} \tag{47}$$

Since

$$\begin{aligned} \bar{y}_2[i] &= (\bar{y}_1[i] - \bar{w}_1[i])e^{j2\pi\varepsilon/2} + \bar{w}_2[i] \\ &= \bar{y}_1[i]e^{j2\pi\varepsilon/2} + (\bar{w}_1[i] - \bar{w}_2[i]e^{j2\pi\varepsilon/2}) \end{aligned} \tag{48}$$

and $\bar{w}_1[i], \bar{w}_2[i]$ are temporally white Gaussian with zero mean and variance $\sigma_w^2 I$, where $\boldsymbol{I}$ is the identity matrix, the multivariate Gaussian vector $\bar{y}_2[i]$ have mean $\bar{y}_1[i]e^{j2\pi\varepsilon/2}$

and covariance matrix

$$E[(\bar{\mathbf{w}}_2[i] - \bar{\mathbf{w}}_1[i]e^{j2\pi\epsilon/2})(\bar{\mathbf{w}}_2[i] - \bar{\mathbf{w}}_1[i]e^{j2\pi\epsilon/2})^H] = 2\sigma_w^2\mathbf{I} \tag{49}$$

Then

$$\begin{aligned} \Lambda(\varepsilon) &= f\left(\bar{y}_1[1]\cdots\bar{y}_1[M_R], \bar{y}_2[1]\cdots\bar{y}_2[M_R] \mid \bar{y}_1[1]\cdots\bar{y}_1[M_R], \varepsilon\right) \\ &\propto \exp\left\{-\frac{1}{2\sigma_\omega^2}\sum_{i=1}^{M_R}\left(\bar{y}_2[i] - \bar{y}_1[i]e^{j2\pi\varepsilon/2}\right)\left(\bar{y}_2[i] - \bar{y}_1[i]e^{j2\pi\varepsilon/2}\right)^H\right\} \\ &\propto \exp\left\{\frac{1}{2\sigma_\omega^2}\sum_{i=1}^{M_R} 2\Re\left\{\bar{y}_2[i]\bar{y}_1^H[i]e^{-j2\pi\varepsilon/2}\right\}\right\} \\ &= \exp\left\{\frac{1}{\sigma_\omega^2}\Re\left\{\left(\sum_{i=1}^{M_R}\sum_{n=1}^{M_R} y_i^*[n]y_i[n+N/2]\right)e^{-j2\pi\varepsilon/2}\right\}\right\} \end{aligned} \tag{50}$$

The ML estimate of ε is given by

$$\begin{aligned} \hat{\epsilon} &= \arg\max_{\epsilon} \Lambda(\epsilon) \\ &= \frac{1}{\pi}\mathrm{Arg}\left(\sum_{i=1}^{M_R}\sum_{n=1}^{N/2} y_i^*[n]y_i[n+N/2]\right) \end{aligned} \tag{51}$$

where Arg(x) is the principal argument of the complex number x. In summary, the generalized Moose estimate for two identical halves pilot symbols of length N_w and N_D-spaced, as shown in Fig. 14, is given by

$$\hat{\epsilon} = \frac{N}{2\pi N_D}\mathrm{Arg}\left(\sum_{i=1}^{M_R}\sum_{n=1}^{N_W} y_i^*[n]y_i[n+N_D]\right) \quad (52)$$

The range of this estimator is $\pm\frac{N}{2N_D}$ sub-carrier spacing.

4.3.2 Extended Yu Estimate

Consider a MIMO-OFDM system that uses multiple identical pilot symbols. After discarding the first received symbol, the remaining K pilot symbols at the *i*th receive antenna, $y_i(k,m)$, can be represented as

$$y_i(k,m) = x_i(k,m) + w_i(k,m) \quad (53)$$

for $k=1,2,\ldots,K$ and $m=1,2,\ldots,M$ where $x_i(k,m)$ is the mth sample of the kth (time-domain) symbol of the channel output at the ith receiver antenna. $\{w_i(k,m)\}$ are uncorrelated circularly symmetric Gaussian random variables at the ith receive antenna with zero mean and variance $\sigma_w^2 = E\left\{\left|w_i(k,m)\right|^2\right\}$. Note that

$$x_i(k,m) = x_1(1,m)e^{j2\pi(k-1)M\varepsilon/N} \quad (54)$$

where ε is the relative frequency offset of the channel. Let

$$\begin{aligned} Y_i(m) &= [y_i(1,m) \cdots y_i(K,m)]^T \\ A(\epsilon) &= \left[1\ e^{j2\pi\epsilon M/N} \cdots e^{j2\pi\epsilon(K-1)M/N}\right]^T \\ W_i(m) &= [w_i(1,m) \cdots w_i(K,m)]^T \end{aligned} \quad (55)$$

where $(.)^T$ denotes the matrix transpose. $Y_i(m), A(\varepsilon)$ and $W_i(m)$ are the vectors of dimension *Kx1*. Then, as shown in Fig 15, we have

$$Y_i(m) = A(\varepsilon)x_i(1,m) + W_i(m), m = 1,\ldots,M \quad (56)$$

The received samples can thus be expressed compactly as

$$Y_i = A(\varepsilon)X_i + W_i \quad (57)$$

where $Y_i = [Y_i(1)\cdots Y_i(M)]$ is an *K*x*M* matrix. $X_i = [x_i(1,1)\cdots x_i(1,M)]$ is an 1xM vector and $W_i = [W_i(1)\cdots W_i(M)]$ is an *K*x*M* matrix. Since the noise is temporally whit Gaussian, $Y_i(m)$ is a multivariate Gaussian distributed random vector with covariance matrix $\sigma_w^2 I$. The joint ML estimates of A and X_i, treating X_i as a deterministic unknown vector, are obtained by maximizing the following joint likelihood function:

$$f\left(Y_1\cdots Y_{M_R} \mid A, X_1\cdots X_{M_R}\right) = \prod_{i=1}^{M_R}\prod_{m=1}^{M} f\left(Y_i(m) \mid A, x_i(1,m)\right)$$
$$\propto e^{-1/\sigma_w^2\sum_{i=1}^{M_R}\sum_{m=1}^{M}\|Y_i(m)-Ax_i(1,m)\|^2}$$

The corresponding log-likelihood function, after dropping constant and unrelated terms, is given by

$$\Lambda\left(A, x_i(1,m)\right) = \sum_{i=1}^{M_R}\sum_{m=1}^{M}\left\|Y_i(m)-Ax_i(1,m)\right\|^2 \quad (58)$$

For a given A, setting $\nabla_{x_i(1,m)}\left\|Y_i(m)-Ax_i(1,m)\right\|^2 = 0$, we obtain the conditional ML estimate, $\hat{x}_i(1,m) = x_{LS_i}(1,m) = A^+Y_i(m)$,where $A^+ = A^H/K$ and H denotes the Hermitian operation. By substituting the least-square solution, $x_{LS_i}(1,m)$, we obtain

$$\begin{aligned} \Lambda(A) &= \sum_{i=1}^{M_R}\sum_{m=1}^{M}\left\|Y_i(m) - AA^+Y_i(m)\right\|^2 = \sum_{i=1}^{M_R}\sum_{m=1}^{M}\left\|P_A^\perp Y_i(m)\right\|^2 \\ &= \sum_{i=1}^{M_R}\sum_{m=1}^{M} Y_i^H(m)P_A^\perp Y_i(m) = tr\left(P_A^\perp\sum_{i=1}^{M_R}\sum_{m=1}^{M}Y_i(m)Y_i^H(m)\right) \\ &= M_R M tr\left(P_A^\perp\hat{R}_{YY}\right) \end{aligned} \quad (59)$$

where $tr(.)$ denotes the trace of a matrix,

$\hat{R}_{YY} = \frac{1}{M_R M}\sum_{i=1}^{M_R}\sum_{m=1}^{M} Y_i(m)Y_i^H(m)$, and $P_A^{\perp} = I - AA^{+}$. The desired CFO estimate is then given by

$$\hat{\varepsilon} = \arg\left\{\min_{\varepsilon} tr\left(P_A^{\perp}\hat{R}_{YY}\right)\right\} = \arg\left\{\max_{\varepsilon} tr\left(P_A\hat{R}_{YY}\right)\right\}$$
$$= \arg\left\{\max_{\varepsilon} A^H\hat{R}_{YY}A\right\} \quad (60)$$

Invoking an approach similar to that used by the MUSIC algorithm, we set $z = e^{j2\pi\varepsilon M/N}$ and define the parametric vector

$$A(z) = \begin{bmatrix}1 & z & z^2 & \cdots & z^{K-1}\end{bmatrix}^T, \quad (61)$$

so that the log-likelihood $\Lambda = A^H\hat{R}_{YY}A$ can be expressed as a polynomial of order *2K-1*,

$$\Lambda(z) = A(z)^H\hat{R}_{YY}A(z) = \sum_{n=-(K-1)}^{K-1} s(n)z^n, \quad (62)$$

where $s(n) = \sum_{i,j}\hat{R}_{YY}(i,j)$, for *n=j-i*, and *n=-K+1,….,K-1*. As the log-likelihood is a real smooth function of ε, taking derivative of $\Lambda\left(e^{j2\pi\varepsilon M/N}\right)$ with respect to ε and setting $\partial\Lambda\left(e^{j2\pi\varepsilon M/N}\right)/\partial\varepsilon = \dot{\Lambda}(\varepsilon) = 0$, we obtain

$$F(z) - F^*(z) = 0 \quad (63)$$

where $F(z) = \sum_{n=1}^{K-1} ns(n)z^n$ is a polynomial of order *K-1*. If $\{z_i\}$ are the nonzero complex roots of $\dot{\Lambda}(z)$ then the desired estimate is given by

$$\hat{\varepsilon} = \frac{N}{j2\pi M}\ln\hat{z} \quad (64)$$

where $\hat{z} = \arg\{\max_{z_i}\Lambda(z)\}$

We summarize the above ML estimation procedure as following.

1. Collect *K* received symbols from all receive antennas and construct the sample correlation matrix $\hat{R}_{YY}$, which is given by $\hat{R}_{YY} = \frac{1}{M_R M}\sum_{i=1}^{M_R}\sum_{m=1}^{M} Y_i(m)Y_i^H(m)$.

2. Calculate the coefficients of *F(z)* based on $\hat{R}_{YY}$ where $F(z) = \sum_{n=1}^{K-1} ns(n)z^n$, and $s(n) = \sum_{i,j}\hat{R}_{YY}(i,j)$ for *n=j-i*.

3. Find the nonzero unit-magnitude roots of $F(z) - F^*(z) = 0$.

4. Obtain the CFO estimate from and $\hat{\varepsilon} = \frac{N}{j2\pi M}\ln\hat{z}$ and $\hat{z} = \arg\{\max_{z_i}\Lambda(z)\}$ where $\Lambda(z) = A(z)^H\hat{R}_{YY}A(z)$, $A(z) = \begin{bmatrix}1 & z & z^2 & \cdots & z^{K-1}\end{bmatrix}^T$, $z = e^{j2\pi\varepsilon M/N}$.

The range of our estimator is subcarrier spacings.

4.4 Simulation Results and Discussion

The computer simulation results reported in this section are obtained by using a pilot format the same as the IEEE 802.11a standard with a sample interval of 50 ns. The frequency-selective fading channel has sixteen paths with independent complex Gaussian distributed amplitudes and a exponentially decaying power delay profile with rms delay spreads of 50 ns. The tap coefficients are normalized such that the sum of the average power per channel is unity. The DFT size is N = 64. The signal-to-noise ratio (SNR), defined as the ratio of the received

signal power (from all MT transmitters) to the noise power at the *i*th receive antenna, is assumed to be the same for each receive antenna. For Moose estimate, the training part consists of two identical halves with length $N_W = 32$. The range of CFO estimator is ± 1 subcarrier spacings. Fig. 16 shows the performance of generalized Moose CFO estimate for different number of transmit and receive antennas. Obviously, the MSE performance improves as the number of receive antennas, M_R, increases. Fig. 17 presents the performance of extended YS estimate for different number of transmit and receive antennas. The training symbol has two identical halves with $K = 2$ and $M = 32$. The range of CFO estimator is ± 1 subcarrier spacings. For training symbol with two identical repetition, the performance of extended Yu estimate is the same as the performance of generalized Moose's CFO estimate. Fig. 18 plots the performance of generalized Moose's CFO estimate with two identical halves with length $N_W = 32$ for different number of transmit and receive antennas. Similarly, the performance of CFO estimates is an increasing function of the number of the receive antennas. We divide roughly into four groups. The first group is $M_R = 1$; $M_T = 1; 2; 4; 8$, the second is $M_R = 2$;$M_T = 1; 2; 4; 8$ and so on. For first group, the performance of CFO estimate with $M_R = 1$; $M_T = 8$ is better than with $M_R = 1$; $M_T = 1$ duo to transmit diversity. The last group with MR = 8 is more close together than the first group with $M_R = 1$ duo to receive diversity. The performance of CFO estimate for the second group, $M_R = 2$, is roughly 3dB better than for the first group, $M_R = 1$, duo to two receive antennas received double energy than single receive antenna. Fig. 19 shows the performance of extended Yu estimate and generalized Moose estimate. The training symbols have 4 repetitions with $K = 4$ and M =16. The training symbols for generalized Moose estimate are length $N_W = 32$ i.e. take first two training symbols as one training symbol and take last two training symbols as one training symbol. The range of generalized Moose's CFO estimator is ± 1 subcarrier spacings. The range of extended Yu estimator is ± 2 subcarrier spacings. For 4 repetitions, the performance of extended YS estimate is better than generalized Moose estimate because extend Yu estimate use all information of training symbols.

4.5 Conclusion

In this project, we have extended both Moose's and Yu's maximum likelihood CFO estimation algorithms for use in MIMO-OFDM systems. As long as the length of cyclic prefix is greater than or equal to the maximum delay that accounts for the all users' timing ambiguities and channel multipath delays. The performance of both CFO estimates improves as the number of transmit/receive antennas increases. In other words, the presence of multiple antennas not only promise great capacity enhancement but entail performance improvement for the associated frequency synchronization subsystem.

5. Reference

[1] S. M. Tseng and M. R. Bell, "Asynchronous multicarrier DS-CDMA using mutually orthogonal complementary

sets of sequences," *IEEE Trans. Commun.,* vol. 48, no. 1, pp. 53-59, Jan. 2000.

[2] C.-M. Yang, G.-C. Yang, P.-H. Lin and W. C. Kwong, "2-D orthogonal spreading codes for multi-carrier DS-CDMA systems," *Proc. of IEEE ICC'03,* May 2003, vol. 5, pp. 3277-3281.

[3] G.-C. Yang and W. C. Kwong, *Prime Codes with Applications to CDMA Optical and Wireless Networks,* Boston, MA: Artech House, 2002.

[4] A. W. Lam and S. Tantaratana, *Theory and Application of Spread Spectrum Systems*. Piscataway, NJ: IEEE, 1994.

[5] M. Pureley, "Performance evaluation for phase-coded spread-spectrum multiple-access communication-Part I: System Analysis," *IEEE Trans. Commun.*, vol. 25, pp. 795-799, Aug. 1977.

[6] M. Pursley and D. Sarwate, "Performance evaluation for phase-coded spread-spectrum multiple-access communication-Part II: Code Sequence Analysis," *IEEE Trans. Commun.*, vol. 25, pp. 800-803, Aug. 1977.

[7] C.-P. Hsieh, C.-Y. Chang, G.-C. Yang, and W.C. Kwong, "A bipolar-bipolar code for asynchronous wavelength-time optical CDMA," to appear *in IEEE Trans. Commun*.

[8] R. A. Monzingo and W. T. Miller, lntroduction to Adaptive Arrays, Wiley, 1980.

[9] S. Haykin, *Adaptive Filter Theory,* Prentice Hall, NJ, 2001.

[10] B. D. V. Veen and K. M. Buckley, "Beamforming: A Versatile Approach to Spatial Filtering," *IEEE ASSP* Mag., pp. 4-24, Apr. 1988.

[11] D. H. Johnson and D. E. Dudgeon, *Array Signal Processing: Concepts and Techniques*, Prentice Hall, 1993.

[12] J. Litva and T. K-Y. Lo, *Digital Beamforming in Wireless Communications*, Artech, 1996.

[13] J. S. Thompson, P. M. Grant, and B. Mulgrew, "Smart Antenna Arrays for CDMA Systems," *IEEE Pers. Commun.*, vol. 3, no. 5, Oct. 1996, pp. 16-25.

[14] Ruly Lai-U Choi, Ross D. Murch, and Khaled Ben Letaief, "MIMO CDMA Antenna System for SINR Enhancement" *IEEE Trans. on Wireless Commun.*, VOL. 2, NO. 2, MARCH 2003

[15] J. C. Liberti and T. S. Rappapor, *Smart Antennas for Wireless Communications: IS-95 and Third Generation CDMA Applications*, Prentice Hall, NJ, 1999.

[16] S. Weinstein, P. Ebert, "Data Transmission by Frequency-Division Multiplexing Using the Discrete Fourier Transform," *IEEE Trans. Commun*., vol. 19, pp. 628 - 634, Oct 1971.

[17] R. van Nee, G. Awater, M. Morikura, H. Takanashi, M. Webster, and K. Halford, "New high-rate wireless LAN standards," *IEEE Commun. Mag*., vol. 37, pp. 82-88, Dec. 1999.

[18] T. Pollet, M. Van Bladel, M. Moeneclaey, "BER sensitivity of OFDM systems to carrier frequency offset and Wiener phase noise," *IEEE Trans. Commun.*, vol. 43, pp. 191-193, Feb./March/April 1995.

6. Tables and Figures

	AWGN	Rician
2-D OVSF	0	$\frac{\sigma^2 MPT_b^{\,2}(K-1)}{N}$
2-D FT	$\frac{M^2 PT_b^{\,2}\overline{\sigma_g^2}}{N^2}$	$\frac{(Mv^2+N\sigma^2)MPT_b^{\,2}\overline{\sigma_g^2}}{N^2}$
2-D Random	$\frac{MPT_b^{\,2}(K-1)}{N}$	$\frac{(v^2+\sigma^2)MPT_b^{\,2}(K-1)}{N}$

*A Rayleigh fading channel is the special case of a Rician fading channel with v=0.

Table I
The variances of MAI of the 2-D FT codes, 2-D OVSF codes and 2-D random codes under the different channels.

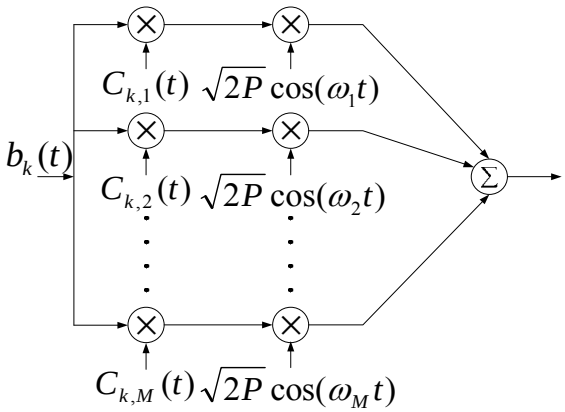

Fig. 1 A transmitter model.

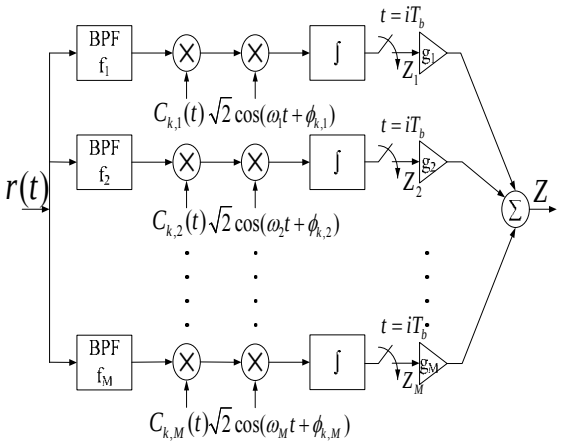

Fig. 2 A receiver model.

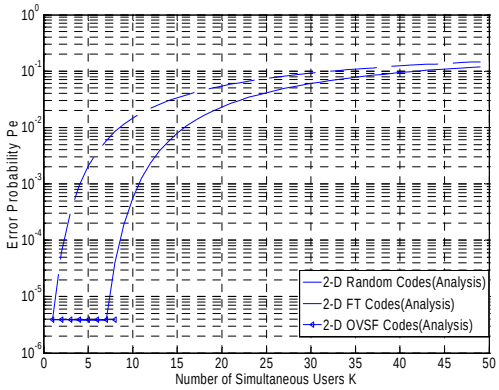

Fig. 3 Error probability P_e versus number of simultaneous users K for the three codes in an AWGN channel (N=7, SNR=10 dB).

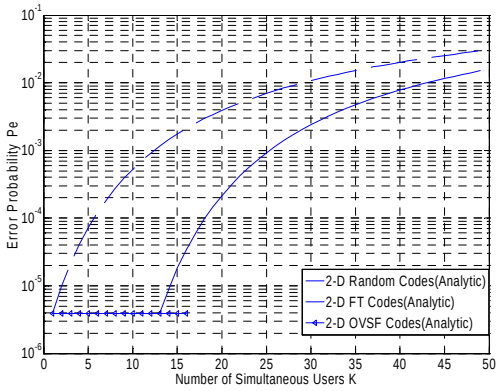

Fig. 4 Error probability P_e versus number of simultaneous users K for the three codes in an AWGN channel (N=13, SNR=10 dB).

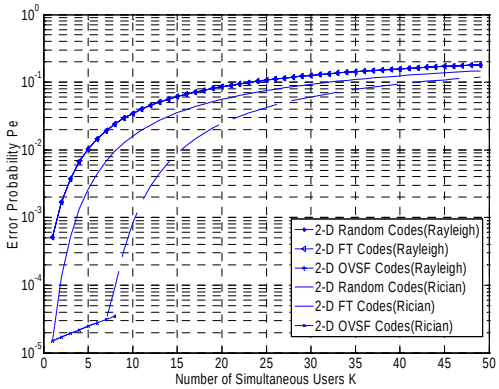

Fig. 5 Error probability P_e versus number of simultaneous users K for the three codes in the strong Rician fading and Rayleigh fading channels (N=7, R=10 dB, SNR=10 dB).

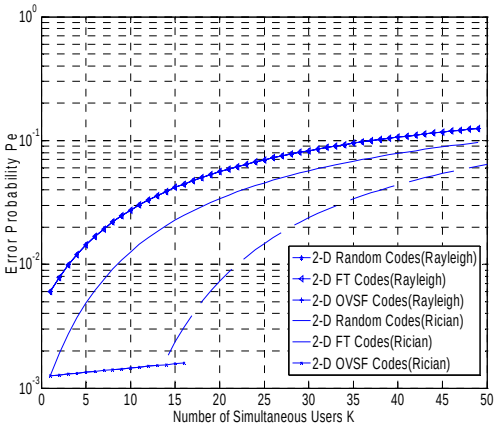

Fig. 6 Error probability P_e versus number of simultaneous users K for the three codes in the strong Rician fading and Rayleigh fading channels (N=13, R=10 dB, SNR=10 dB).

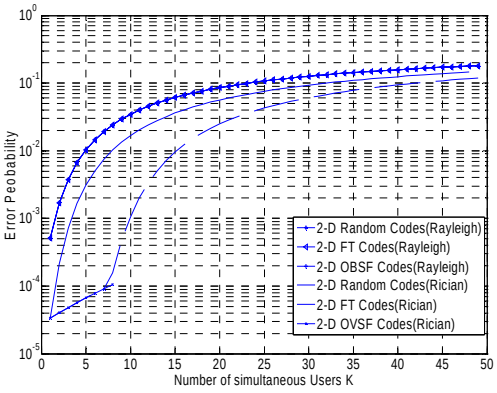

Fig. 7 Error probability P_e versus number of simultaneous users K for the three codes in the weak Rician fading and Rayleigh fading channels (N=7, R=5 dB, SNR=10 dB).

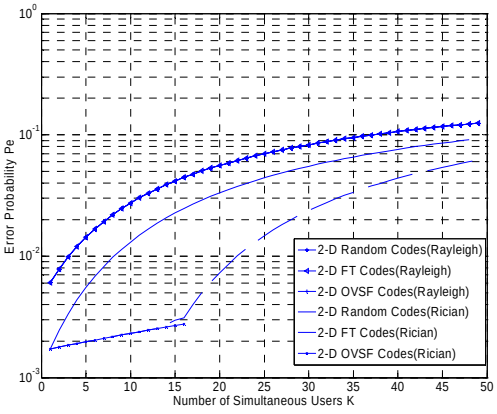

Fig. 8 Error probability P_e versus number of simultaneous users K for the three codes in the weak Rician fading and Rayleigh fading channels (N=13, R=5 dB, SNR=10 dB).

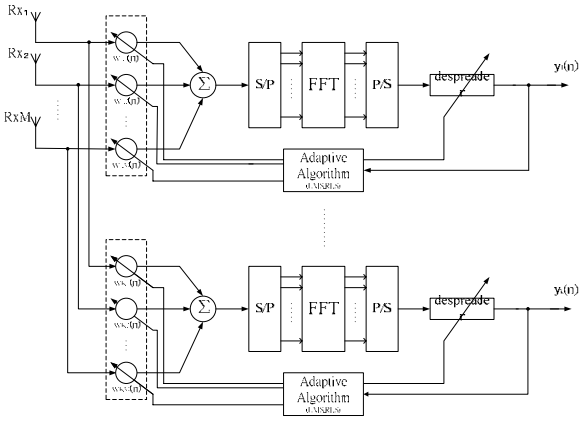

Fig. 9 MIMO-OFDM-DS/CDMA Receiver Structures

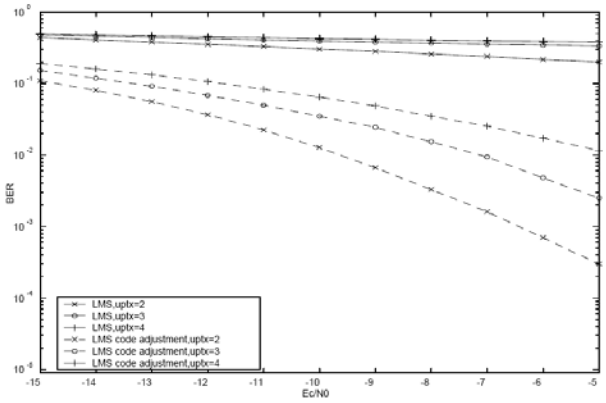

Fig. 10 BER performance of narrowband LMS-based adaptive receiver with different user number in each transmitted antenna branch.

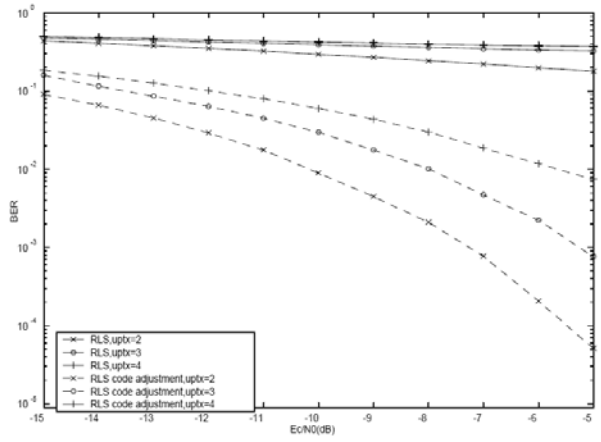

Fig. 11 BER performance of narrowband RLS-based adaptive receiver with different user number in each transmitted antenna branch.

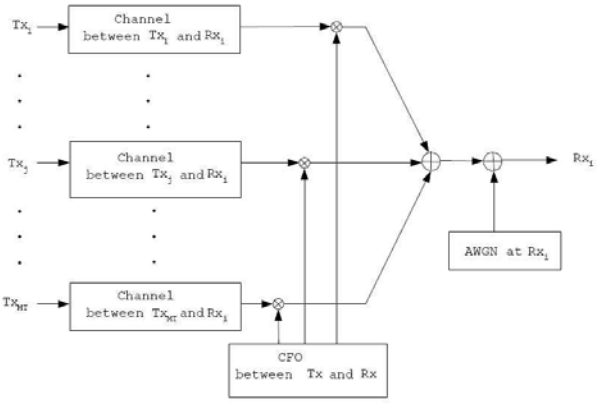

Fig. 12 Channel model for the ith receive antenna.

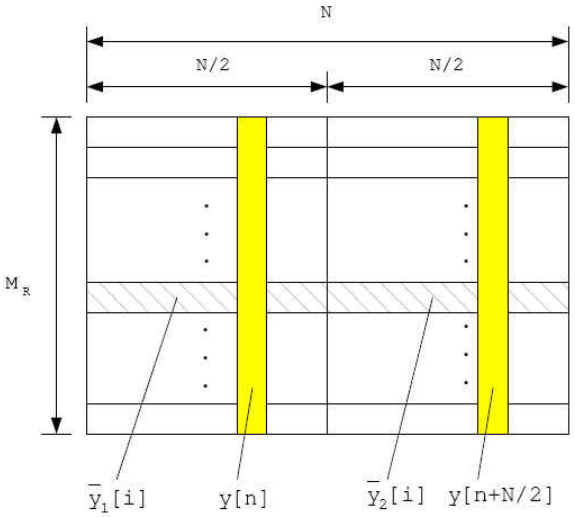

Fig. 13 Definitions of various vector notations.

Fig. 14 The ND-spaced estimator.

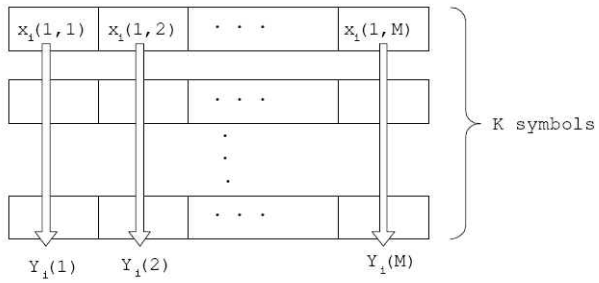

Fig. 9 Symbol arrangement and definitions of the extended Yu's ML estimate at the *i*th receive antenna.

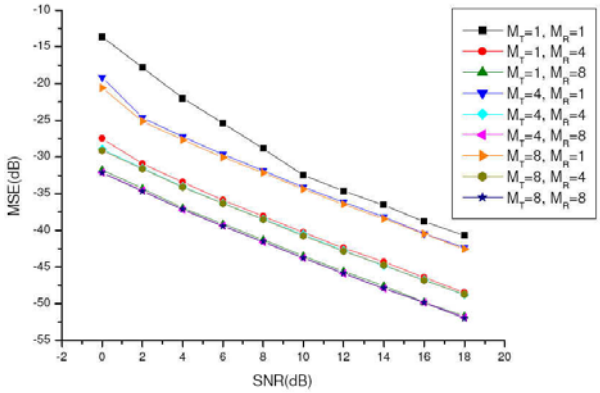

Fig. 10 MSE performance of generalized moose estimate for two repetitions, true CFO = 0:7 subcarrier spacings.

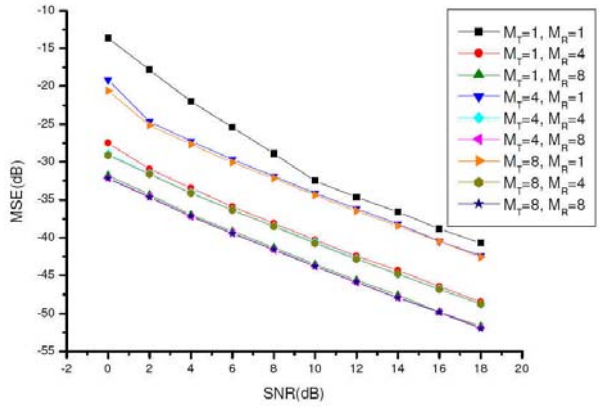

Fig. 11: MSE performance of extended Yu estimate for two repetitions, true CFO=0:7 subcarrier spacings.

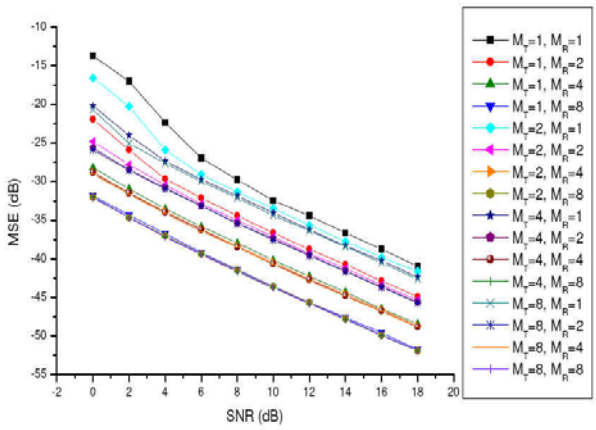

Fig. 12: MSE performance of generalized moose estimate for two repetitions, true CFO=0:7 subcarrier spacings.

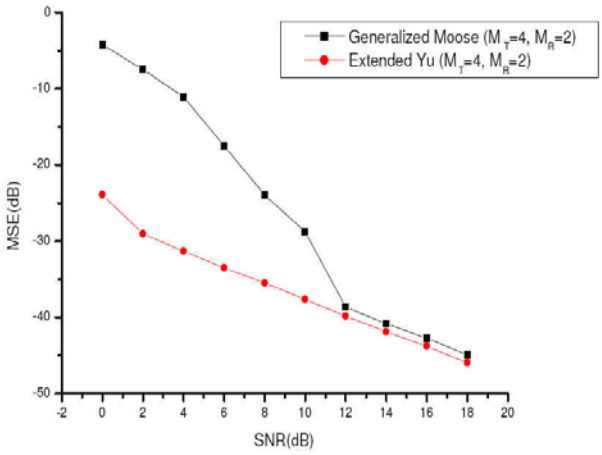

Fig. 13: MSE performance of CFO estimates for four repetitions, true CFO = 0:93 subcarrier spacings.